Article

JOURNAL OF UNIVERSITY OF BABYLON
For Pure and Applied Sciences (JUBPAS)

Vol.31; No.3.| 2023

The Optimizing of Prefabricated Solar Cells by Dual Plasmonic Nanoparticles

Baraa Hussam |Ali*[1] , Lazem H. Aboud[2] , Mohammed J. Jader[3]

1College of science for women University of Babylon, baraahussam886@gmail.com, Hilla , Iraq .
2College of science for women, University of Babylon, wsci.lazem.hussan@uobabylon.edu.iq, Hilla , Iraq.
3College of science for women, University of Babylon, wsci.mohammed.jawad@uobabylon.edu.iq , Hilla , Iraq.

***Corresponding author email:** baraahussam886@gmail.com ; mobile: +9647827644370

تحسين الخلايا الشمسية المحضرة مسبقا بواسطة جسيمات نانوية بلازمونية مزدوجة

براء حسام علي [1*]، لازم حسن عبود[2]، محمد جواد جادر [3]

1 كلية العلوم للبنات ، جامعة بابل ، : baraahussam886@gmail.com ، صندوق بريد4- مدينة الحلة ، الحلة ، العراق

2 كلية العلوم للبنات ، جامعة بابل ، wsci.lazem.hussan@uobabylon.edu.iq ، الحلة ، العراق

3 كلية العلوم للبنات ، جامعة بابل ، wsci.mohammed.jawad@uobabylon.edu.iq ، الحلة ، العراق

Accepted: 28 /7 /2023 **Published:** 30 /9 /2023

ABSTRACT

Background: The quest for improving the efficiency of solar cells has garnered considerable attention in numerous scientific investigations. One promising approach involves utilizing plasmons generated by metal nanoparticles to enhance the performance of photovoltaic solar cells.

Materials and Methods: High-purity gold nanoparticles (AuNPs), silver nanoparticles (AgNPs), and a combination of both were synthesized using pulsed laser ablation in distilled water. Subsequently, these nanoparticles were deposited onto silicon (Si) substrates and pre-existing Si homo-junction photovoltaic cells.

Results: The optical analysis of the prepared nanoparticle suspension revealed distinct plasmonic bands located at approximately 400 nm and 523 nm wavelengths for AgNPs and AuNPs, respectively. In the case of the AuNPs:AgNPs mixture, two plasmonic bands were observed, corresponding to the presence of both types of metal nanoparticles. The X-ray diffraction (XRD) analysis of the deposited nanoparticle samples on Si wafers demonstrated a polycrystalline structure for all samples. Scanning electron microscopy (SEM) imaging displayed uniformly distributed spherical Au nanoparticles on the substrate, while AgNPs exhibited some aggregations.

Conclusion: The photovoltaic (PV) solar cells demonstrated an enhanced performance, attributed to the ability of the plasmonic nanoparticles to facilitate increased light absorption or enhance surface conductivity. The combination of silver and gold particles holds promise for solar surface coating, further optimizing the cells to capture a greater amount of solar radiation within their plasmon peaks. This study highlights the potential of plasmonic nanoparticles to enhance the efficiency of previously prepared PV cells.

Key words: Solar Cells , Plasmonic Nanoparticles , AgNPs, AuNPs.

ISSN: 2312-8135 | Print ISSN: 1992-0652 | www.journalofbabylon.com | jub@itnet.uobabylon.edu.iq | info@journalofbabylon.com

ISSN: 2312-8135 | Print ISSN: 1992-0652
info@journalofbabylon.com | jub@itnet.uobabylon.edu.iq | www.journalofbabylon.com

INTRODUCTION

The increase in the global demand for energy as well as the emergence of the problem of environmental pollution led to the urge to search for alternatives energy resources to fossil fuels [1]. Photovoltaic solar cells (PV) is one of the most important alternative sources of renewable energy gaining global attention in numerous application fields [2]. As the surface area occupied by photovoltaic cells, increasing the efficiency of solar photon harvesting is a major concern of many researchers working in this field [3]. The efficiency of solar cells based on semiconductor materials is limited due to high optical and electrical losses by recombination processes [4]. The plasmonic light trapping technology is regarded as one of the promising technologies in recent years [4]. Plasmonic of noble metal nanoparticles like metal nanoparticles such as gold, silver, etc. can interact with photons whose frequency is matched by the resonance of collective oscillation electrons within the nanoparticles [5]. So, deposited on a semiconductor surface introduce a unique behaviour by responding to incident light at a specific range, the metal islands present a resonant absorption of light corresponding to the oscillation of collective behaviour of free charges in these islands. In the light interacted with plasmonic particles causes cumulative oscillations of the confined electrons in the NPs cause to modify the electrical field intensity around them which enhance the photo electron generations. Furthermore, the light trapped by scattering from the plasmonic nanoparticles inside the active layer causes to improve light absorption [6]. These nanoparticles properties can be tuned to harvest sun light at specific range of the spectrum. Moreover, the plasmonic NPs suggest an effective way to reduce the absorber film thickness, and increase the conductivity which causes to reduce the recombination process [7].

Numerous studies have proposed different techniques for enhance harvesting sunlight inside the PV devise with the use of anti-reflection coatings [8], grids in windows [9], and by plasmon nanoparticles [10]. The best technique for PV enhancing the localized light absorption is by the plasmonic approach using different plasmonic metals nanoparticles such as Ag, Au, Cu, etc [11][12], which can tuned by varying the nanoparticles shapes [13]

The incorporation of plasmonic nanoparticles into PV cell causes an increasing of light absorption by light-trapping, and increase the generated electron-hole pairs by enhancing a localized field by electromagnetic, and fast injection of electrons into semiconductor which reduces the recombination process [14]. The two main categories of light-trapping techniques are, decreasing the top surface's reflection coefficient and lengthening the optical path within the cell by multiple scattering using the localized surface plasmon resonant particles [15]. Au and Ag act as an effective scattering element to capture more photons and thus, a higher J_{sc} as well, as a higher efficiency of solar cell that can be can achieved [16].

Behera et al, (2022) studied the improvement of optical and electrical characteristics of Cu_2ZnSnS_4 (CZTS) solar cells through incorporating Ag nanoparticles. AgNPs were stacked using sputtering DC technique. Regular distribution of Ag NPs was achieved. The concentration

of Ag was varied by varying the deposition time. The optical property of CZTS films was enhanced by the Ag nanoparticles. The resistivity decreased by increasing the deposited NPs concentration. Zhu et al, (2023) [17] improved the efficiency of GaAs thin-film solar cell with TiO_2 nano plasmonic pyramids and Ag NPs. The Ag NPs extends the optical path of incident light cause multiple absorptions within the cell caused to enhance its efficiency.

In this paper we present one possible way to increase the efficiency of previously prepared photovoltaic cells of silicon homojunction by using nano-dimensional islands of gold, silver and their mixed.

MATERIALS AND METHODS

A pulsed Nd-YAG laser of 1064 nm wavelength, pulse width of 10 ns, repetition frequency of 4 Hz and pulse energy of 100 mJ was in laser ablation technique to produce AuNPs, and AgNPs in distilled water. The laser was focused using a fluorescence lens, with a focal length of (10 cm) on the sample immersed into 10 ml distilled water.

The Si is immersed in the prepared solutions of the two metal nanoparticles and their mixture for 120 seconds and extracted for 60 seconds at a temperature of 80 °C, and by repeated for 5 times to obtain nanoparticles layers. The optical properties of the prepared nanoparticles and the mixed samples suspension in distilled water were examined by studying its absorbance using UV-visible type (CECIL 7200) spectrophotometer. The structural properties of the prepared nanoparticle samples deposited on Si wafer were examined using the X-ray diffraction (Shimadzu XRD 6000).

A previously manufactured homo-junction Si solar cell coated by TiO_2 as antireflection was used. The cells were etched by 1:10 diluted HF acid for 10 min to remove the TiO2 coating. The suspension samples of AuNPs, AgNPs, and AuNPs:AgNPs were deposited on silicon bases and the surface of solar cell by a dip coating device at 80 °C. A compensation TiO_2 film was deposited onto the cell by thermal evaporation under high vacuum using Edward coating system. The schematic diagram of the controlled and plasmonic enhanced PV cells were shown in Figure 1. The J-V characteristics were measured by a Keithley electrometer under the light radiation source of 100 mW/cm^2. The same procedure was followed for the plasmonic enhanced PV cells.

ISSN: 2312-8135 | Print ISSN: 1992-0652
info@journalofbabylon.com | jub@itnet.uobabylon.edu.iq | www.journalofbabylon.com

ISSN: 2312-8135 | Print ISSN: 1992-0652
info@journalofbabylon.com | jub@itnet.uobabylon.edu.iq | www.journalofbabylon.com

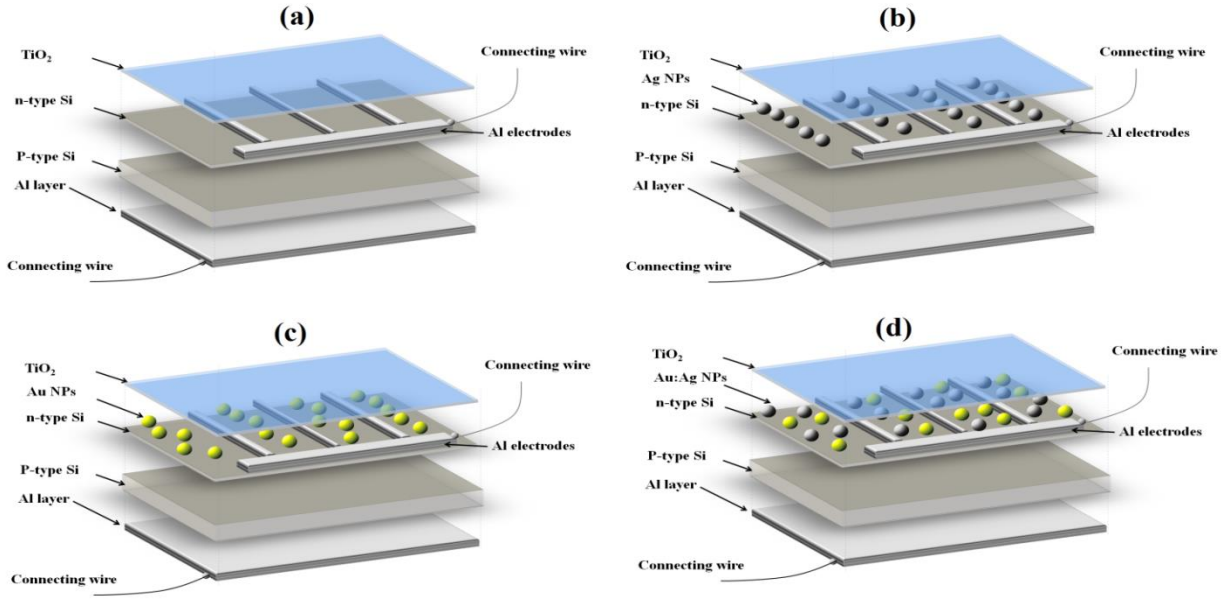

Fig. 1. Solar cell configurations of (a) bare, (b)Ag catted, (c)Au catted, (d)Au:Ag coated.

RESULTS AND DISCUSSION

The XRD patterns for AuNPs, AgNPs, and AuNPs:AgNPs deposited on a (100) Si wafer, compared with the standard cards, were shown in Figure 2. Polycrystalline structure with four peaks for each sample located around diffraction angles of 2θ= 38 °, 44 °, 64.5°, and 77.5° corresponding to crystalline planes (111), (200), (220), and (311) according to No. 96-901-2954 and 96-901-2432 standard cards, corresponding to Au and Ag structures, respectively. The addition intense diffraction peak corresponding to the (100) Si substrate located at diffraction angle 69°. It is worth mentioning here that the standard lines for both gold and silver were very close due to the similarity in the crystal structure of the two metals and their possession of a close lattice constants values.

The interspacing distances (d_{hkl}) were determined according to Bragg's formula [18]:

$$n\lambda = 2d_{hkl}\sin\theta \quad \text{.....1}$$

while the crystallite size (C.S) calculated according to Debye–Scherrer formula [19]:

$$D = \frac{0.94\,\lambda}{\beta\,\mathrm{Cos}\theta} \quad \text{.....2}$$

Table 1lists the structural parameters for the AuNPs, AgNPs, and AuNPs:AgNPs mixture deposited on Si wafer. The d_{hkl} values were close to the standard ones. The results showed that crystal size of the obtained NPs have small dimensions of average value (12.1, 10.9, and 11.9) nm for the AgNPs, AuNPs, and their mixture, respectively. The resulting nanomaterial's can be used in modern applied fields.

ISSN: 2312-8135 | Print ISSN: 1992-0652
info@journalofbabylon.com | jub@itnet.uobabylon.edu.iq | www.journalofbabylon.com

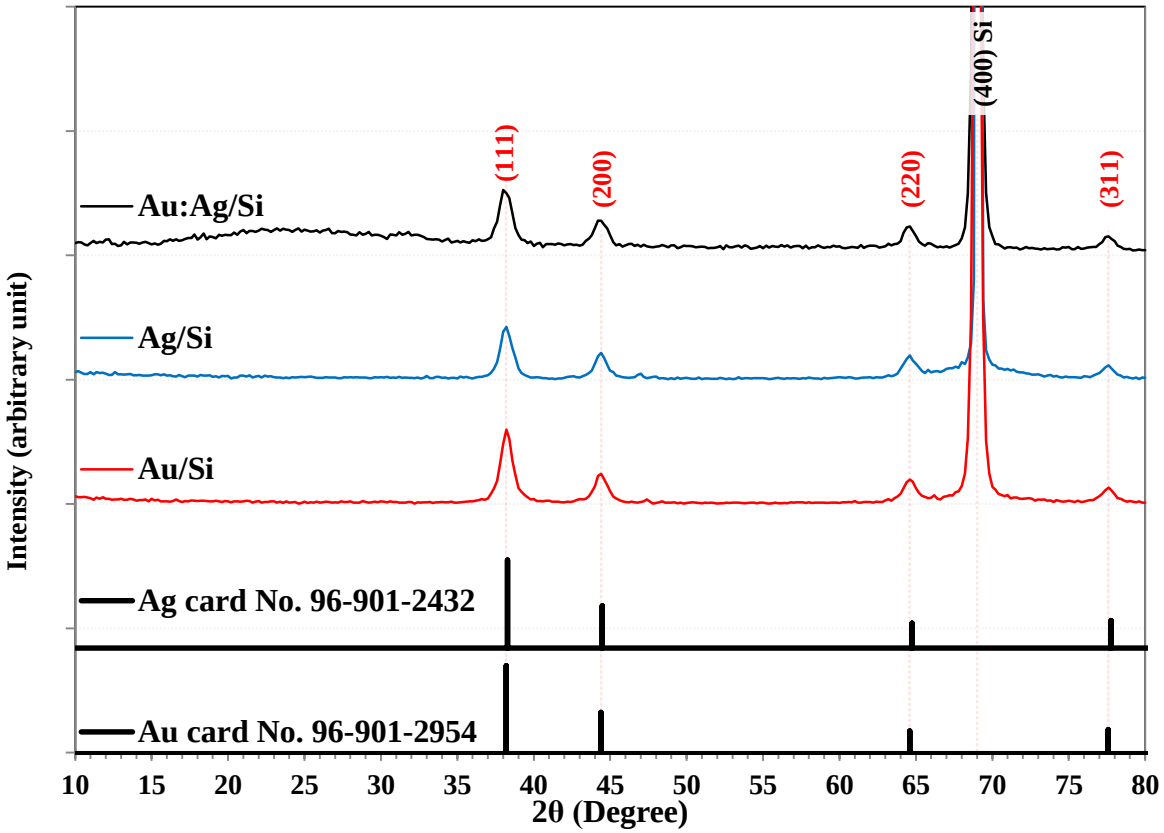

Figure 2. XRD for Ag Coated, Au Coated Au:Ag Coated Si Compared with the Standard Lines

Table 1. XRD Parameters for AuNPs/Si, AgNPs/Si, and Au:AgNPs/Si.

Sample	2θ (Deg.)	FWHM (Deg.)	d_{hkl} Exp.(Å)	C.S (nm)	Phase	hkl
AuNPs /Si	38.3301	0.8502	2.3464	9.9	Cub. Au	(111)
	44.3124	0.8752	2.0425	9.8	Cub. Au	(200)
	64.5285	0.8251	1.4430	11.4	Cub. Au	(220)
	77.5933	0.8251	1.2294	12.4	Cub. Au	(311)
AgNPs /Si	38.1925	0.7802	2.3545	10.8	Cub. Ag	(111)
	44.4499	0.6601	2.0365	13.0	Cub. Ag	(200)
	64.5285	0.7701	1.4430	12.2	Cub. Ag	(220)
	77.5933	0.8251	1.2294	12.4	Cub. Ag	(311)
AuNPs:AgNPs /Si	38.0550	0.7630	2.3627	11.0	Au:Ag	(111)
	44.2436	0.7441	2.0455	11.5	Au:Ag	(200)
	64.5285	0.6602	1.4430	14.2	Au:Ag	(220)
	77.5933	0.9351	1.2294	10.9	Au:Ag	(311)

Figure 3 displays the top view of FESEM images, at two magnification powers of 200.0 kX, for the AuNPs, AgNPs, and AuNPs:AgNPs deposited on Si wafer, and next to their granulate cumulating number percentage distribution for NPs diameters determined by ImageJ software. The AgNPs have spherical shapes of 22.69 nm diameter, but with some aggregations of about

200 nm diameter. Wide particle size distribution from 13 to 39 nm was appeared. These aggregations were occurred due to the oxidization capability of silver metal. The AuNPs appeared to have spherical shapes uniformly sprayed over the surface of narrow distribution from 13 to 29 nm of 19.49 nm average diameter. The image of mixed sample consists the two shapes of nanoparticles. The distribution appeared as double modes, for the mixed particles, centered around 10 and 23 nm diameters. The average particle diameter was 12.42 nm.

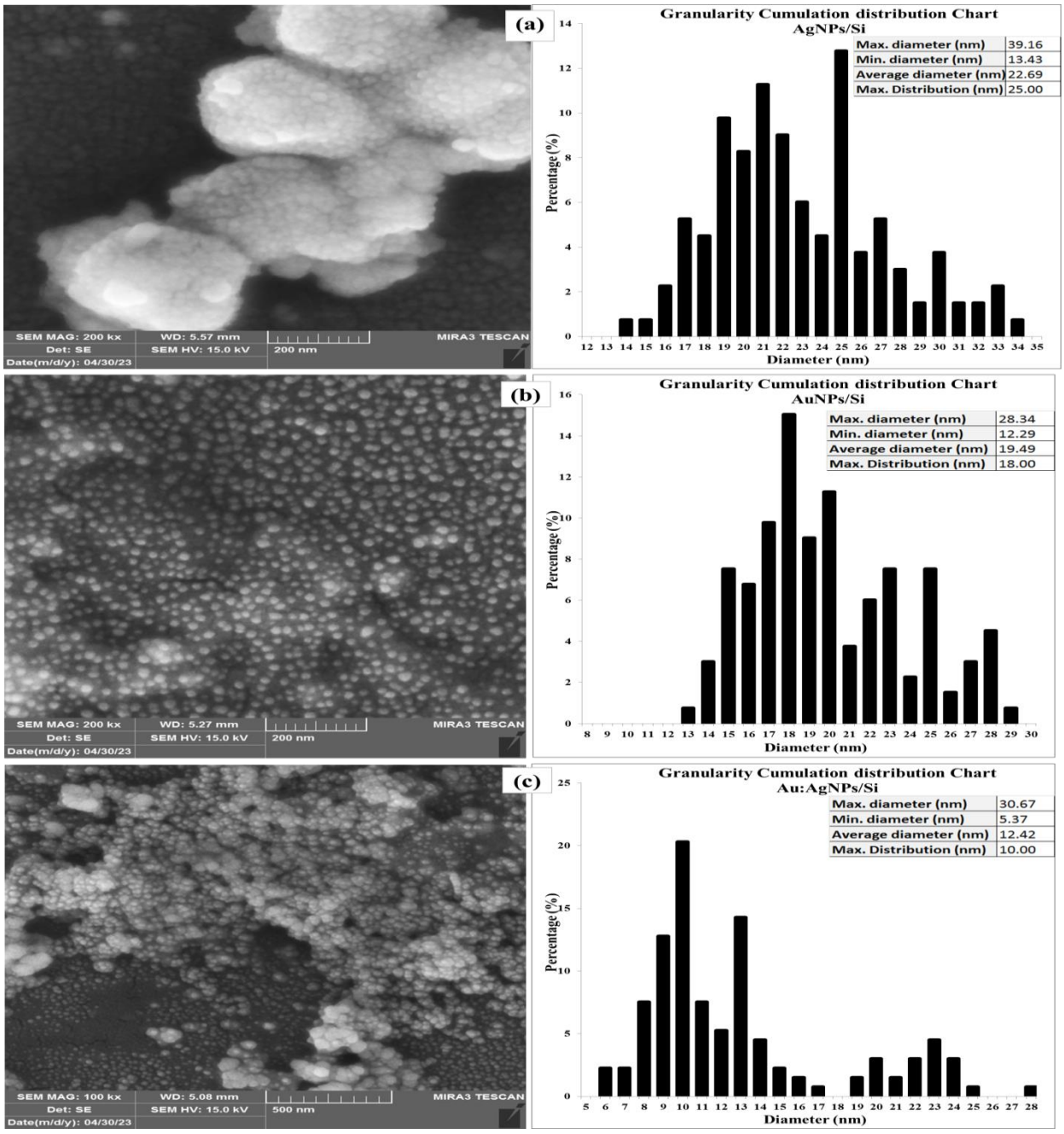

Figure 3. FE-SEM images for a)Ag coated, (b)Au coated, (c)Au:Ag coated Si.

ISSN: 2312-8135 | Print ISSN: 1992-0652
info@journalofbabylon.com | jub@itnet.uobabylon.edu.iq | www.journalofbabylon.com

ISSN: 2312-8135 | Print ISSN: 1992-0652
info@journalofbabylon.com | jub@itnet.uobabylon.edu.iq | www.journalofbabylon.com

The optical absorbance spectra of the AgNPs, AuNPs, and Au:AgNPs suspensions in distilled water prepared by pulsed laser ablation were shown in Figure 5. The absorption curve for the AgNPs, show a plasmonic band located around 398 nm wavelength, which is the characteristics LSPR band for AgNPs [20]. The optical absorbance spectra of the AuNPs show a plasmonic band located around 523 nm wavelength, which is the characteristics LSPR band for AuNPs [21]. The optical absorbance spectra of the AuNPs:AgNPs mixture in distilled water appeared with doubled bands corresponding to the two types of the metal NPs for the LSPR. This mixture can be used to tune the absorbance to wide spectral range. Table 2 lists the LSPR wavelength and the maximum absorbance for the AgNPs, AuNPs, and AuNPs:AgNPs suspensions.

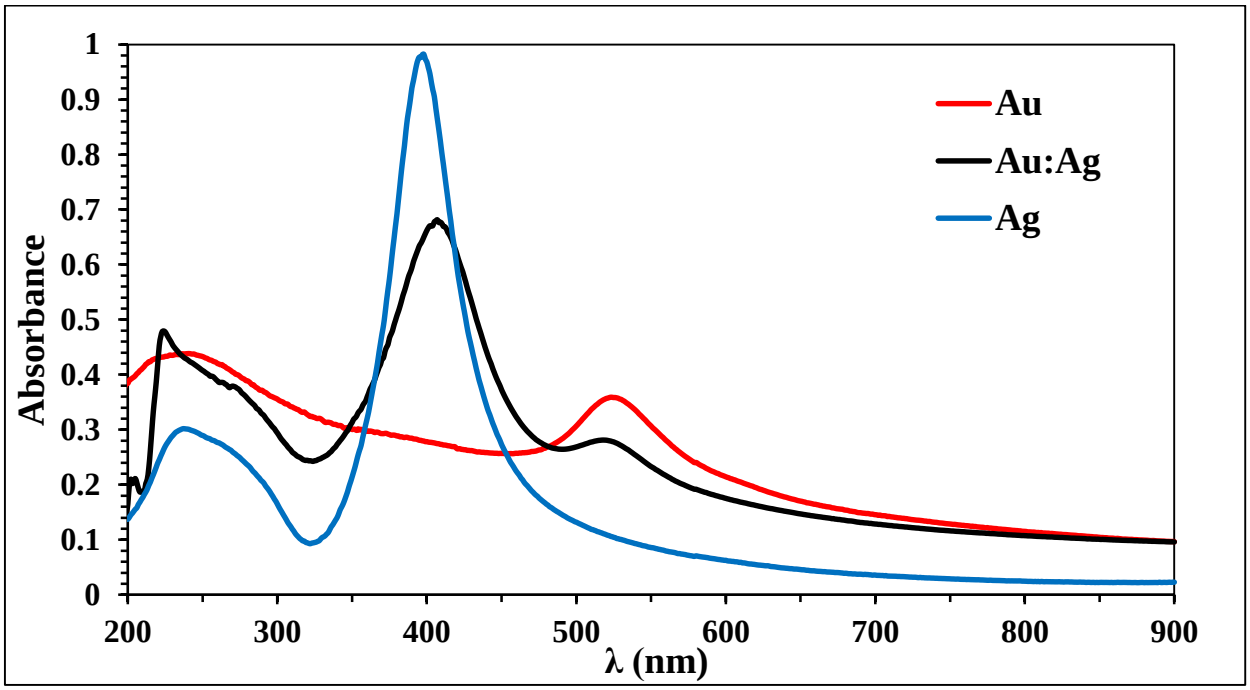

Figure 4. Absorption Curves for AgNPs, AuNPs, and Ag:AuNPs Colloidal

Table 2. Plasmon Peaks Wavelength and their Maximum absorbance for for AgNPs, AuNPs, and Ag:AuNPs Colloidal

.Sample	λ (nm)	Absorbance	λ (nm)	Absorbance
Au NPs	-	-	523	0.359
Ag NPs	398	0.982	-	-
Au:Ag NPs	407	0.682	518	0.281

Figures 5 to 8 show the current density –voltage (J-V), and power–voltage characteristics (P-V) for a commercial homojunction P-Si/n-Si under illumination of (100 mW/cm^2) by a halogen lamp, which simulate the sunlight irradiance. The sample exhibits photovoltaic effect with cross area in the fourth quarter of J-V curve. The maximum power showed as the area of the rectangle drawn inside the cross area. The open circuit voltage was 0.65 V and the short circuit

current density 4.40 mA/cm^2. The fill factor and maximum conversion efficiency are calculated as follow:

$$FF = \frac{I_m V_m}{I_{sc} V_{oc}} \quad \text{.....5}$$

$$\eta_{max} = \frac{P_m}{P_{in}} \times 100\% \quad \text{.....6}$$

$I_m, V_m, I_{sc}, and\ V_{oc}$ represent the current and voltage at maximum power P_m, short current circuit and open circuit voltage. The maximum harvesting power was 1.64 mW per centimeter square at 0.4 V. The maximum power represent as an area of the rectangle drawn inside the cross area of $P_m=J_m \times V_m$. The final efficiency was 1.36%, while the shunt resistance (R_{sh}) and series resistance (R_s) were 181.36, and 52.45 Ω, respectively.

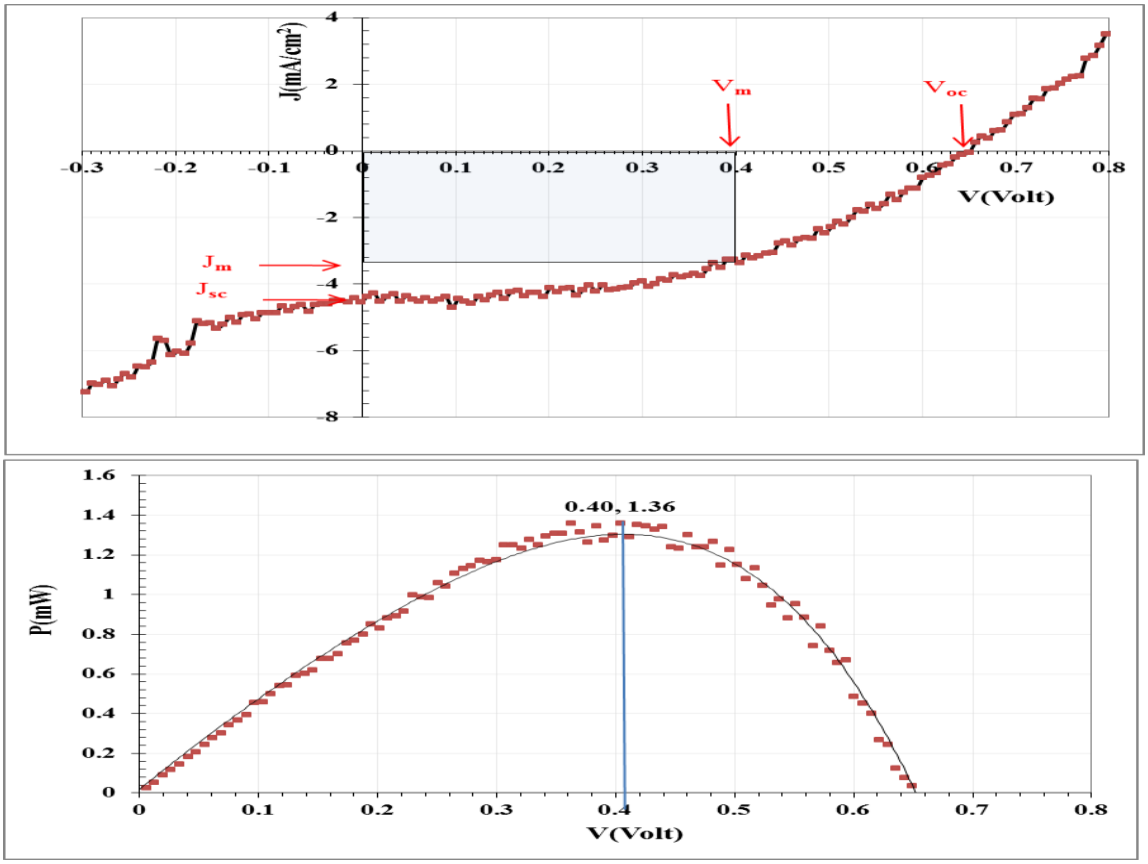

Figure 5. J-V and P-V curves for the pure solar cell

ISSN: 2312-8135 | Print ISSN: 1992-0652
info@journalofbabylon.com | jub@itnet.uobabylon.edu.iq | www.journalofbabylon.com

ISSN: 2312-8135 | Print ISSN: 1992-0652
info@journalofbabylon.com | jub@itnet.uobabylon.edu.iq | www.journalofbabylon.com

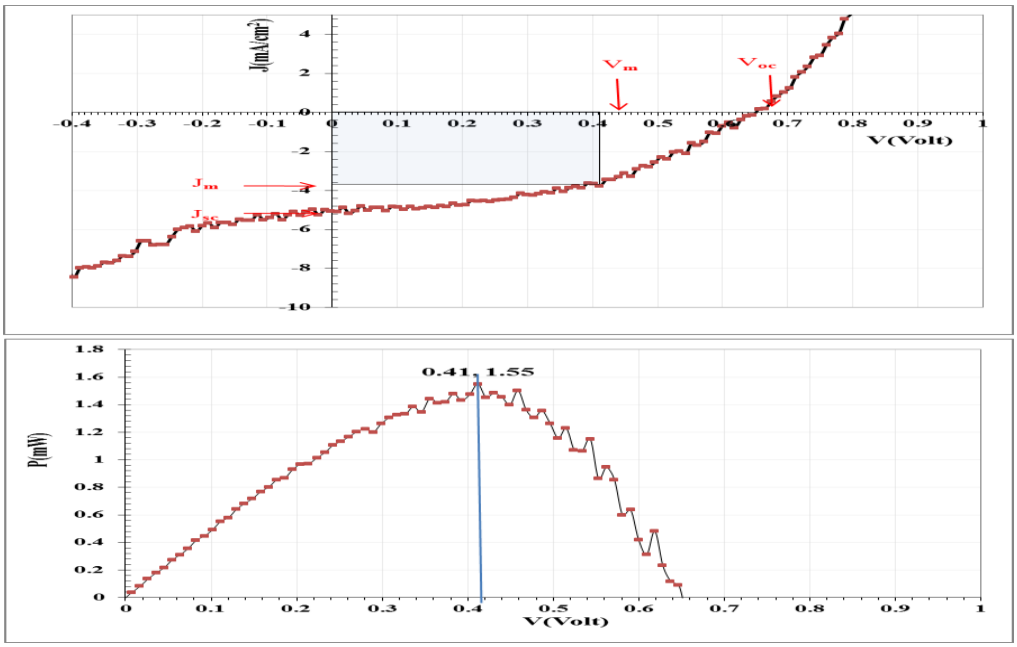

to Figure show the current J-V, and P-V curves for coated solar cells by AuNPs, AgNPs and their mixture under illumination of 100 mW/cm^2. All samples exhibit photovoltaic effect with cross area in the fourth quarter of J-V cure. By comparing the results with the untreated sample, it is noted that there was no change in the open circuit voltage value, while the short circuit current values increased, but with varying degrees. The increasing of I_{sc} values is due to the presence of metal particles, which is done by two mechanisms: the first is due to the increase in absorption due to the scattering that occurs on the surface of the cell, which leads to photon trapping inside the cell, and increases the absorption process[22]. The second is enhancing the solar cell efficiency by the LSPR effect, which cause accelerated separated charge and rapid injection of electrons into semiconductor materials, so, lowered recombination rate [23]. Increment in photocurrent may assign to helpful injection of hot electrons by SPR effect [22].

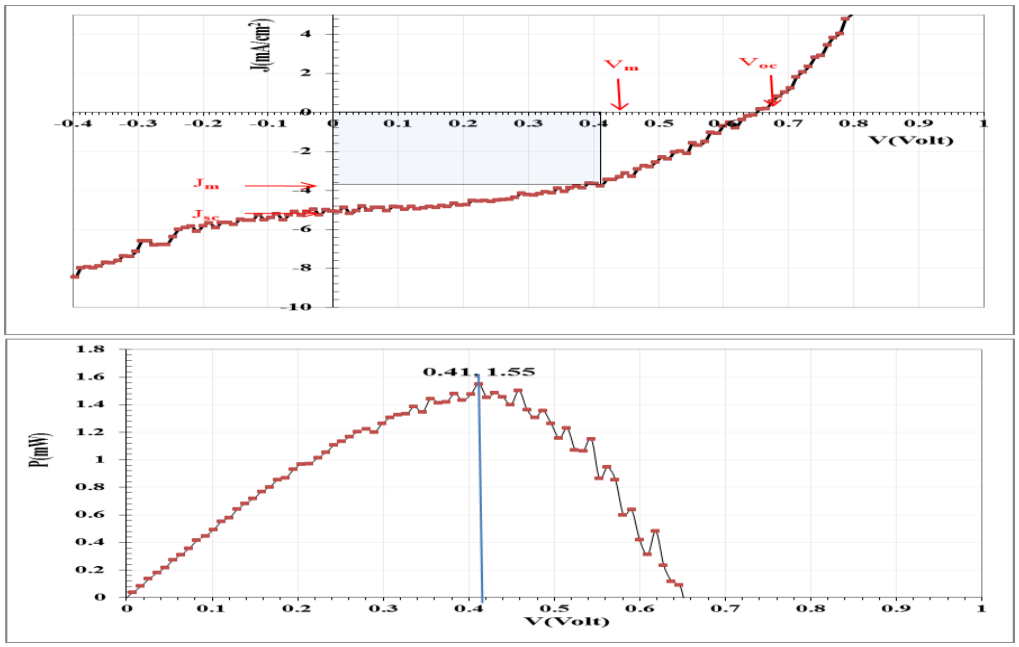

Figure 6. J-V and P-V Curves for the PV Cell Coated by AgNPs

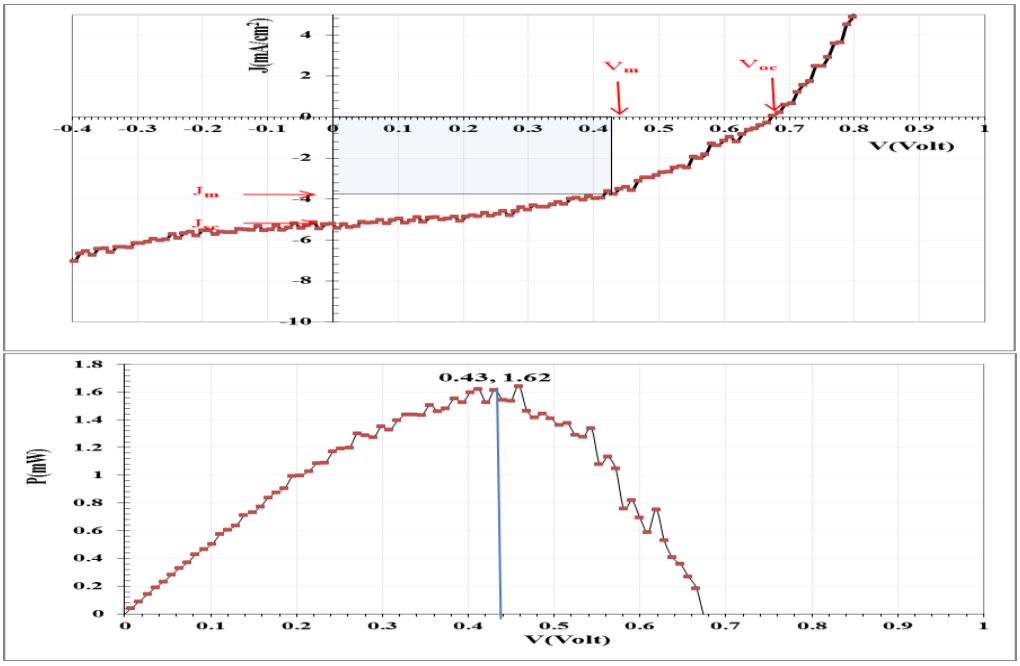

Figure 7. J-V and P-V Curves for the PV Cell Coated by AuNPs

ISSN: 2312-8135 | Print ISSN: 1992-0652
info@journalofbabylon.com | jub@itnet.uobabylon.edu.iq | www.journalofbabylon.com

ISSN: 2312-8135 | Print ISSN: 1992-0652
info@journalofbabylon.com | jub@itnet.uobabylon.edu.iq | www.journalofbabylon.com

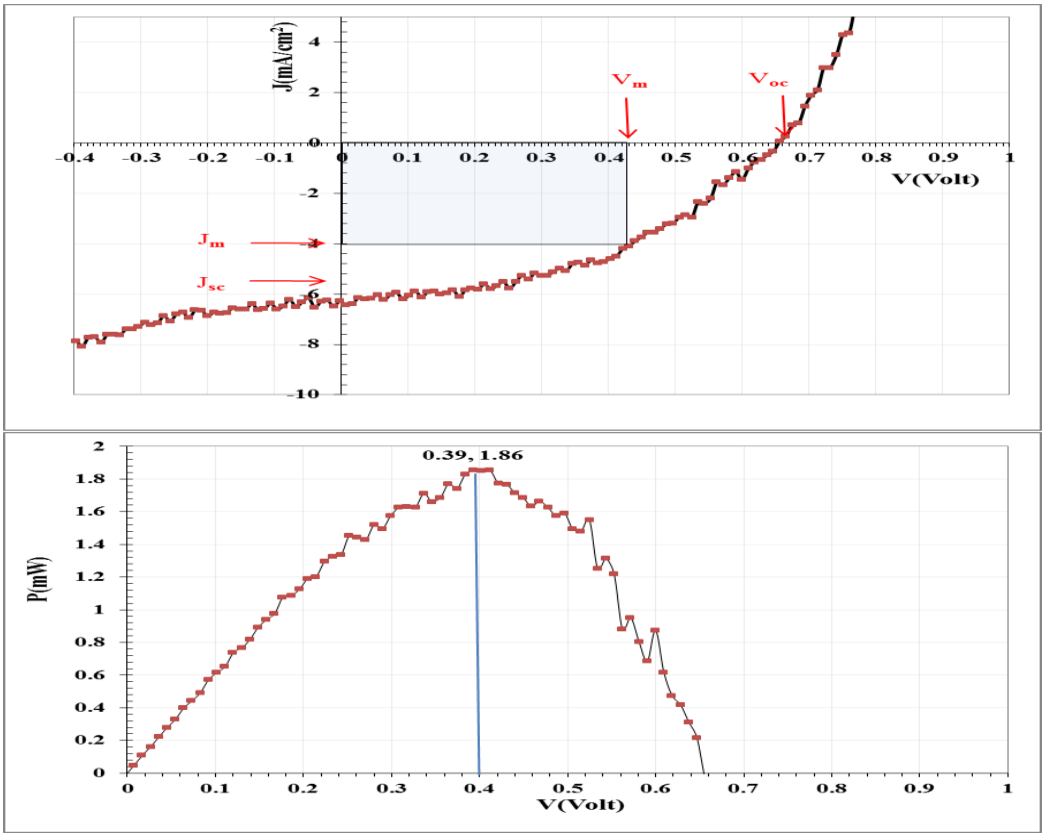

Figure 8. J-V and P-V Curves for the PV Cell Coated by AuNPs:AgNPs Mixture

The solar cell characteristics including the open-circuit voltage (V_{oc}), short-circuit current (J_{sc}), fill factor (FF), and solar efficiency (η) for these cells for the bare solar cell and that enhanced with the nanoparticles are summarized in Table 3. The quantum efficiency increased from 1.36% for the controlled cell to 1.55%, 1.62% and 1.89% for the PV cell coated by AuNPs, AgNPs, and AuNPs: AgNPs, respectively. The higher efficiency for the cell coated by the mixed NPs due to the two ranges of absorption for the two NPs types which cause the harvesting of more solar energy [24]. Increasing the shunt resistance for the PV cell enhanced by NPs indicates the reduction of the recombination rate of the generated electron-hall pairs [25]. The solar cell more enhanced in efficiency with Au NPs than the AgNPs as their variation in plasmonic wavelength which falls about at the middle of spectral maximum causees more light harvesting. In addition, using mixed nanoparticles, causes more enhancement due to the contribution of two absorption bands corresponding to the two NPs [24]. For all coatings, the shunt resistance increased while the series resistance decreased indicating on increase in the electron injection conductivity and reducing the recombination process [25].

Table 3. The Specification of Solar Cell before and after the Treatment with AgNPs, AuNPs, and AuNPs:AgNPs Mixture.

	Bare	With AgNPs	With AuNPs	With AuNPs:AgNPs
J_{sc} (mA)	4.40	5.00	5.20	6.40
V_{oc} (V)	0.65	0.65	0.67	0.65
J_m (mA)	3.40	3.78	3.77	4.85
V_m(v)	0.40	0.41	0.43	0.39
F.F	0.48	0.48	0.46	0.45
η%	1.36	1.55	1.62	1.89
R_{sh} (Ω)	181.36	394.16	339.56	234.74
R_s (Ω)	52.45	33.03	34.21	23.81

CONCLUSIONS

High purity AuNPs and AgNPs were simply prepared by pulsed laser ablation technique. The XRD patterns for AuNPs, AgNPs, and AuNPs:AgNPs deposited on a (100) Si wafer shows polycrystalline structure for the all samples. The FE-SEM of the deposited AuNPs on Si wafer appeared as spherical shapes of 13.9 nm diameter uniformly deposited on the substrate. While the AgNPs appeared as aggregations of about 200 nm diameter. The LSPR bands of AuNPs and AgNPs locate in the visible region of the solar spectrum. Depositing the metal nanoparticles onto a previously prepared solar cells can enhanced their performance to harvest more energy by increasing the absorption inside the active layer at the plasmonic wavelength or by reducing the recombination process by increasing surface conductivity. It is possible to take advantage of mixing silver and gold particles to use them for solar surface coating to further improve the cells to capture a larger amount of solar radiation, because each of them contributes to enhancing the optical absorption within its plasmon peak.

ACKNOWLEDGMENTS:

Authors would thank College of science for women, University of Babylon for their support.

ISSN: 2312-8135 | Print ISSN: 1992-0652
info@journalofbabylon.com | jub@itnet.uobabylon.edu.iq | www.journalofbabylon.com

Conflict of interests.

The authors declare that they have no conflict of interest.

References

[1] W. J. Ho, J. C. Chen, J. J. Liu, and C. H. Ho, "Enhancing luminescent down-shifting of Eu-doped phosphors by incorporating plasmonic silver nanoparticles for silicon solar cells," *Appl. Surf. Sci.*, vol. 532, no. May, p. 147434, 2020.

[2] A. A. Qureshi, S. Javed, H. M. A. Javed, A. Akram, M. S. Mustafa, U. Ali, and M. Z. Nisar, "Facile formation of SnO2–TiO2 based photoanode and Fe3O4@rGO based counter electrode for efficient dye-sensitized solar cells," *Mater. Sci. Semicond. Process.*, vol. 123, p. 105545, 2021.

[3] P. Mandal, "Application of Plasmonics in Solar Cell Efficiency Improvement: a Brief Review on Recent Progress," *Plasmonics*, vol. 17, no. 3, pp. 1247–1267, 2022.

[4] A. Axelevitch, B. Gorenstein, and G. Golan, "Application of gold nano-particles for silicon solar cells efficiency increase," *Appl. Surf. Sci.*, vol. 315, no. 1, pp. 523–526, 2014.

[5] M. Seyyedi and H. Heidarzadeh, "Comparative study of a perovskite solar cell using different aperiodic arrangements of plasmonic nanoparticles," *Opt. Mater. (Amst).*, vol. 135, p. 113287, 2023.

[6] T. Shahabi, H. Heidarzadeh, and H. Bahador, "Dual metallic-based plasmonic back reflector to broaden the absorption spectra of a thin film amorphous silicon solar cell," *Opt. Commun.*, vol. 544, p. 129623, 2023.

[7] G. Chen, J. Seo, C. Yang, and P. N. Prasad, "Nanochemistry and nanomaterials for photovoltaics," *Chem. Soc. Rev.*, vol. 42, no. 21, pp. 8304–8338, 2013.

[8] A. A. Tabrizi and A. Pahlavan, "Efficiency improvement of a silicon-based thin-film solar cell using plasmonic silver nanoparticles and an antireflective layer," *Opt. Commun.*, vol. 454, p. 124437, 2020.

[9] R. Saive, "Light trapping in thin silicon solar cells: A review on fundamentals and technologies," *Prog. Photovoltaics Res. Appl.*, vol. 29, no. 10, pp. 1125–1137, 2021.

[10] T. Shen, S. Siontas, and D. Pacifici, "Plasmon-Enhanced Thin-Film Perovskite Solar Cells," *J. Phys. Chem. C*, vol. 122, no. 41, pp. 23691–23697, 2018.

[11] N. Behera and B. M. D., "Investigation of broad-band optical absorption and electrical properties in vacuum annealed CZTS/Ag multi-layered stack structure for plasmonic solar cell application," *Opt. Mater. (Amst).*, vol. 127, p. 112316, 2022.

[12] M. Li, N. Yuan, Y. Tang, L. Pei, Y. Zhu, J. Liu, L. Bai, and M. Li, "Performance optimization of dye-sensitized solar cells by gradient-ascent architecture of SiO2@Au@TiO2 microspheres embedded with Au nanoparticles," *J. Mater. Sci. Technol.*, vol. 35, no. 4, pp. 604–609, 2019.

[13] Z. Samavati, A. Samavati, A. F. Ismail, A. Awang, E. S. Sazali, M. Velashjerdi, and Eisaabadi B, "Influence of Ag NPs shape and metal oxide shell embedded in the active layer of Si-based hybrid plasmonic solar cells on device efficiency," *Phys. Scr.*, vol. 98, no. 5, p. 055506, 2023.

[14] X. He, Y. Guo, X. Li, and J. Liu, "In situ ligand-free growth of TiO2-escapsulated Au nanocomposites on photoanode for efficient dye sensitized solar cells," *Chem. Eng. J.*, vol. 396, p. 125302, 2020.

[15] W.-Y. Rho, D. H. Song, H.-Y. Yang, H.-S. Kim, B. S. Son, J. S. Suh, and B.-H. Jun, "Recent advances in plasmonic dye-sensitized solar cells," *J. Solid State Chem.*, vol. 258, pp. 271–282, 2018.

[16] M. Guo, J. Chen, J. Zhang, H. Su, L. Liu, N. Fu, and K. Xie, "Coupling plasmonic nanoparticles with TiO2 nanotube photonic crystals for enhanced dye-sensitized solar cells performance," *Electrochim. Acta*, vol. 263, pp. 373–381, 2018.

[17] J. Zhu, G. Jin, and L. Qin, "High-efficiency and cost-effective manufacturing of solar cells based on

ISSN: 2312-8135 | Print ISSN: 1992-0652
info@journalofbabylon.com | jub@itnet.uobabylon.edu.iq | www.journalofbabylon.com

localized surface plasmonic resonance," *Opt. Mater. (Amst).*, vol. 141, p. 113897, 2023.

[18] L. K. Dintle, P. V. C. Luhanga, C. Moditswe, and C. M. Muiva, "Compositional dependence of optical and electrical properties of indium doped zinc oxide (IZO) thin films deposited by chemical spray pyrolysis," *Phys. E Low-dimensional Syst. Nanostructures*, vol. 99, pp. 91–97, 2018.

[19] M. O. Salman, M. A. Kadhim, and A. A. Khalefa, "CdO : SnO 2 Composite UV-Assisted Room Temperature Ozone Sensor," *Iraqi J. Sci.*, vol. 64, no. 3, pp. 1190–1202, 2023.

[20] C.-C. Huang, H.-J. Chen, Q. L. Leong, W. K. Lai, C.-Y. Hsu, J.-C. Chen, and C.-L. Huang, "Synthesis of silver nanoplates with a narrow LSPR band for chemical sensing through a plasmon-mediated process using photochemical seeds," *Materialia*, vol. 21, p. 101279, 2022.

[21] V. Gupta, A. Srivastava, R. Jain, V. K. Sharma, and L. Kumar, "Optimization and development of ITO-free plasmonic gold nanoparticles assisted inverted organic solar cells," *Opt. Mater. (Amst).*, vol. 131, p. 112747, 2022.

[22] V. S. Manikandan, A. K. Palai, S. Mohanty, and S. K. Nayak, "Surface plasmonic effect of Ag enfold ZnO pyramid nanostructured photoanode for enhanced dye sensitized solar cell application," *Ceram. Int.*, vol. 44, no. 17, pp. 21314–21322, 2018.

[23] Q. Liu, Y. Wei, M. Z. Shahid, M. Yao, B. Xu, G. Liu, K. Jiang, and C. Li, "Spectrum-enhanced Au@ZnO plasmonic nanoparticles for boosting dye-sensitized solar cell performance," *J. Power Sources*, vol. 380, pp. 142–148, 2018.

[24] T. Solaiyammal and P. Murugakoothan, "Green synthesis of Au and the impact of Au on the efficiency of TiO2 based dye sensitized solar cell," *Mater. Sci. Energy Technol.*, vol. 2, no. 2, pp. 171–180, 2019.

[25] W.-Y. Rho, H.-S. Kim, W.-J. Chung, J. S. Suh, B.-H. Jun, and Y.-B. Hahn, "Enhancement of power conversion efficiency with TiO2 nanoparticles/nanotubes-silver nanoparticles composites in dye-sensitized solar cells," *Appl. Surf. Sci.*, vol. 429, pp. 23–28, 2018.

ISSN: 2312-8135 | Print ISSN: 1992-0652
info@journalofbabylon.com | jub@itnet.uobabylon.edu.iq | www.journalofbabylon.com

ISSN: 2312-8135 | Print ISSN: 1992-0652
info@journalofbabylon.com | jub@itnet.uobabylon.edu.iq | www.journalofbabylon.com

الخلاصة

المقدمة: حظي السعي لتحسين كفاءة الخلايا الشمسية باهتمام كبير في العديد من التحقيقات العلمية. يتضمن أحد الأساليب الواعدة استخدام البلازمونات الناتجة عن الجسيمات النانوية المعدنية لتحسين أداء الخلايا الشمسية الكهروضوئية.

طرق العمل: تم تصنيع جسيمات الذهب النانوية عالية النقاء (AuNPs) وجسيمات الفضة النانوية (AgNPs) ومزيج من كليهما باستخدام الاستئصال بالليزر النبضي في الماء المقطر. بعد ذلك ، تم ترسيب هذه الجسيمات النانوية على ركائز السيليكون (Si) والخلايا الكهروضوئية المتجانسة Si المحضرة مسبقًا.

النتائج: أظهر التحليل البصري لمعلق الجسيمات النانوية المحضرة نطاقات بلازمونية مميزة تقع عند حوالي 400 نانومتر و 523 نانومتر من الأطوال الموجية للفضة النانوية والذهب النانوي، على التوالي. بينما في حالة الخليط ، لوحظ وجود قمتين بلازمونية ، يتوافقان مع وجود كلا النوعين من الجسيمات النانوية المعدنية. أظهر تحليل حيود الأشعة السينية (XRD) لعينات الجسيمات النانوية المودعة على رقائق Si بنية متعددة البلورات لجميع العينات. عرض التصوير بالمجهر الإلكتروني (SEM) الجسيمات النانوية الكروية الموزعة بشكل موحد على الركيزة ، بينما أظهرت دقائق الفضة بعض التجمعات.

الخلاصة: أظهرت الخلايا الشمسية الكهروضوئية أداءً معززًا ، يُعزى إلى قدرة الجسيمات النانوية البلازمية على تسهيل زيادة امتصاص الضوء أو تعزيز التوصيل السطحي. إن الجمع بين جزيئات الفضة والذهب يفتح الافاق لطلاء سطوح الخلايا الشمسية ، مما يؤدي إلى زيادة تحسين الخلايا لالتقاط قدر أكبر من الإشعاع الشمسي بواسطة قمم البلازمون الخاصة بها. تسلط هذه الدراسة الضوء على إمكانات الجسيمات النانوية البلازمونية لتعزيز كفاءة الخلايا الكهروضوئية المعدة مسبقًا.

الكلمات المفتاحية: **الخلايا الشمسية ، الجسيمات النانوية البلازمونية ، جسيمات الفضة النانوية ، جسيمات الذهب النانوية**